ELSEVIER

Journal of Molecular Catalysis A: Chemical 153 (2000) 199–207

JOURNAL OF MOLECULAR CATALYSIS A: CHEMICAL

www.elsevier.com/locate/molcata

Oxidative dehydrogenation of ethane on Cr, mixed Al/Cr and mixed Ga/Cr oxide pillared zirconium phosphate materials

B. Solsona [a], J.M. López-Nieto [a], M. Alcántara-Rodríguez [b], E. Rodríguez-Castellón [b], A. Jiménez-López [b,*]

[a] *Instituto de Tecnología Química, UPV-CSIC, Avda. Los Naranjos s / n. 46022 Valencia, Spain*
[b] *Departamento de Química Inorgánica, Facultad de Ciencias, Universidad de Málaga, 29071 Málaga, Spain*

Received 22 June 1999; accepted 13 September 1999

Abstract

Cr-containing oxide pillared zirconium phosphate materials have been synthesized using the fluorocomplex method. They are active catalysts for the oxidation of ethane but present a low selectivity to ethene. In these materials the partial substitution of Cr cations by Ga or Al decreases the catalytic activity but increases the selectivity to ethene. The effect of the substitution of Cr^{3+} by Ga^{3+} or Al^{3+} on the selectivity to ethene during the oxidation of ethane can be related to the modification of both the oxidizing power and the acid strength of active sites. In this way, the higher the substitution of Cr the lower is both the oxidizing power of Cr cations and the acid strength of acid sites. The better selectivity to ethene was obtained on Ga/Cr-containing materials with a Ga/(Cr + Ga) atomic ratio of 0.4.

Keywords: Oxidative dehydrogenation of ethane; Cr-, Ga/Cr- and Al/Cr-containing pillared zirconium phosphate

1. Introduction

One of the key points of the technology for the oxidative dehydrogenation of alkanes is the development of catalysts capable of activating only the C–H bonds of alkanes in a flow of O_2. Vanadium and molybdenum oxides are the most commonly used active phases supported on a varied group of materials such as SiO_2 [1], MgO [2–4], Al_2O_3 [5], TiO_2 [6,7], $AlNbO_4$ [5], sepiolite [8], TiO_2/SiO_2 [9], TiO_2/Al_2O_3 [10], calcined hydrotalcite [11], microporous aluminophosphates [4,12], and vanadium-substituted aluminophosphates [4,13]. Recently different reviews on this reactions appeared in the literature [14,15].

The effectiveness of these supported catalysts depends upon the dispersion degree of the active phase. One method to obtain highly dispersed oxides is by pillaring. Pillared layered structures (PLS) derived from layered materials such as metal(IV) layered phosphates have attracted interest and recent reviews pointed out their potential applications in catalysis [16,17]. These solids are composed of metal (Al, Zr, Cr) oxide nanoclusters which prop the layer permanently apart, giving rise to porous thermally stable materials. Chromia pillared α-zirconium phosphate exhibits a good activity and selectiv-

* Corresponding author.

1381-1169/00/$ - see front matter
PII: S1381-1169(99)00346-5

ity in the thiophene hydrodesulfurization reaction [18] and is also active in the dehydrogenation of propane [19]. Since Cr(III) can form stable solid solutions with other trivalent cations such as Al and Ga, it is also possible to obtain mixed metal (Al/Cr, Ga/Cr) oxide pillared α-zirconium phosphates with variable M(III)/Cr(III) ratios [20,21], where Ga/Cr oxide pillared α-zirconium phosphate is an acid catalyst active in the vapour-phase deep oxidation of halohydrocarbons [21] and in the propane dehydrogenation reaction [22]. For the later reaction, this catalyst is very active and stable, especially under oxidative conditions.

Cr-containing catalysts are active in the oxidative dehydrogenation (OXDH) of ethane and propane [23–26], although one of the best catalysts is characterized by the presence of Cr^{3+} incorporated on zirconium hydrogenophosphates [25,26].

The aim of this paper is to study the catalytic behavior in the oxidative dehydrogenation of ethane of a group of catalysts based on chromia pillared α-zirconium phosphate in which we have also introduced Ga^{+3} in different loadings and Al^{+3} ions as dopant in order to know their influence on the activity and selectivity in such oxidative reaction.

2. Experimental

2.1. Preparation of pillared phosphates

The host material, α-zirconium phosphate (α-ZrP), was synthesized using the fluorocomplex method [27]. A colloidal suspension of α-ZrP was prepared by exposing the phosphate to *n*-propylamine vapors overnight. After removing the excess *n*-propylamine in a desiccator with concentrated phosphoric acid, the solid was dispersed in 0.03 M acetic acid and the pH was adjusted to 8 with a solution 0.1 M *n*-propylamine. This colloidal suspension was contacted with the following:

(1) Ga/Cr–ZrP catalysts. Three pillaring solutions, containing a total amount of Ga^{3+} and Cr^{3+} equal to 10 times the cationic exchange capacity of the α-ZrP (6.64 meq g^{-1}), and with Ga/Cr molar ratios of 30/70, 40/60 , and 70/30. The mixtures were refluxed for 2 days. The pillaring solutions were prepared by dissolving $Ga(NO_3)_3 \cdot 9H_2O$ and $Cr(NO_3)_3 \cdot 9H_2O$ in water. The pH was maintained at 4.4–4.5 by adding *n*-propylammonium acetate (0.1 M) and *n*-propylamine. The OAc^-/Cr^{3+} molar ratio was 2.8. The preparation and full characterization of pillared materials were described elsewhere [21]. After reaction, the solids were separated by centrifugation, washed with deionized water until a conductivity < 50 μS of the washing water was obtained, dried in air at 125°C for 1 day and finally calcined at 400°C flowing N_2 for 12 h.

(2) AlCr–ZrP catalyst. The 40/60 Al/Cr–ZrP sample was prepared applying the same conditions previously described for Ga/Zr–ZrP samples, but using $Al(NO_3)_3 \cdot 9H_2O$ as Al source [20].

(3) Cr–ZrP sample. The chromia–ZrP catalyst was prepared using a 0.031 M chromium(III) acetate aqueous solution (25 mmol of Cr^{3+}/g α-ZrP). The mixture was refluxed for 4 days. After reaction, the green solid was recovered by centrifugation, rinsed three times with deionized water, and dried at 60°C [28]. Finally, the catalyst was treated on similar conditions to that of mixed metal oxide-pillared α-zirconium phosphate. Table 1 summarizes the most relevant characteristics of these solids.

2.2. Characterization

Chemical analysis of gallium, aluminium and zirconium were done by atomic absorption (AA) spectroscopy. Chromium was determined colorimetrically as chromate ($\lambda = 372$ nm) after treatment of the samples with $NaOH/H_2O_2$. The water content was determined by thermal analysis with a Rigaku Thermoflex instrument (calcined Al_2O_3 was used as reference and the heating rate was 10 K min^{-1}). The acetate content was determined by CHN analysis.

Table 1
Chemical compositions, textural and acidic properties of catalysts

Catalyst	Chemical analysis		XPS Cr/Zr atomic ratio	S_{BET} ($m^2\ g^{-1}$)	$V_{micropore}$ ($cm^3\ g^{-1}$)	NH_3-TPD ($\mu mol\ g^{-1}$)	Py-IR Lewis ($\mu mol\ g^{-1}$)		2-C_3H_8OH decomposition (μmol propeno $g^{-1}\ s^{-1}$)
	% Cr	% Ga or Al					100°C	220°C	
Ga/Cr-0/100	39.7	0	4.56	426	0.25	2350	542	497	17.4
Ga/Cr-30/70	30.6	14.1	4.05	326	0.12	2020	434	382	15.0
Ga/Cr-40/60	21.1	21.0	3.51	283	0.12	1751	413	340	13.7
Ga/Cr-70/30	11.5	39.7	1.63	257	0.09	1633	211	147	13.9
Al/Cr-40/60	17.4	10.1	1.60	295	0.14	1395	312	280	Nd

Nitrogen adsorption and desorption isotherms were determined in a conventional volumetric apparatus at 77 K and after degassing the samples at 200°C (1.33×10^{-2} Pa, overnight).

X-ray photoelectron spectroscopy (XPS) analyses were obtained using a Physical Electronics 5700 instrument with Al Kα and Mg Kα X-ray excitation sources ($h\nu = 1486.6$ and 1253.6 eV, respectively) and hemispherical electron analyser. Accurate (± 0.01 eV) binding energies (BEs) were determined with respect to the position of the C_{1s} peak at 284.8 eV. The residual pressure in the analysis chamber was maintained below 10^{-7} Pa during data acquisition. Each spectral region of photoelectron interest was scanned several times to obtain good signal-to-noise ratios.

Ammonia thermal programmed desorption (NH_3-TPD) was used to determine the total acidity of the samples. Before the adsorption of ammonia at 100°C, the samples were heated at 400°C in an He flow. The NH_3-TPD was performed between 100° and 400°C, with a heating rate of 10°C min^{-1}, and analysed by on-line gas chromatograph (Shimadzu GC-14A) provided with a TC detector.

IR of adsorbed pyridine (Py-IR) spectra were recorded on a Perkin-Elmer 883 spectrometer. Self-supported wafers of the samples with a weight/surface ratio of about 12 mg cm^{-2} were placed in a vacuum cell with greaseless stopcocks and CaF_2 windows. The samples were evacuated at 350°C and 10^{-2} Pa overnight, exposed to pyridine vapors for 15 min and then outgassed at room temperature, 100°C, 220°C and 350°C. The IR spectra of the calcined materials with adsorbed pyridine shows the characteristic bands of pyridine interacting with both Lewis and Brönsted acid centers. The band at 1550 cm^{-1} is assigned to the pyridinium ion formed on a Brönsted acid site, while the band at 1450 cm^{-1} corresponds to the pyridine coordinated to Lewis acid centers. The concentrations of both types of acid sites were estimated for the integrated absorption at 1550 and 1450 cm^{-1}, using the extinction coefficients obtained by Dakta et al. [29], $E_B = 0.73$ cm μmol^{-1} and $E_L = 1.11$ cm μmol^{-1}, for Brönsted and Lewis sites, respectively.

Isopropanol decomposition was tested in a fixed-bed tubular glass microreactor at 350°C and atmospheric pressure using about 30 mg of catalyst with dilution. The isopropanol was fed into the reactor by bubbling a flow of He through a saturator-condenser at 30°C, which allowed a constant flow of 25 ml min^{-1} with 7.4% of isopropanol and spatial velocity of 41 mol $g^{-1}\ s^{-1}$. Before the catalytic test, the samples were pretreated at 220°C in He flow for 2 h and then kept for 1 h at 220°C under static He atmosphere. The gas carrier was passed through a molecular sieve trap before being saturated with isopropanol. The reaction products were analysed by on-line gas chromatograph provided with an FID and a fused silica capillary column SPB1.

Thermal programmed reduction (TPR) was performed between 40°C and 720°C, using a

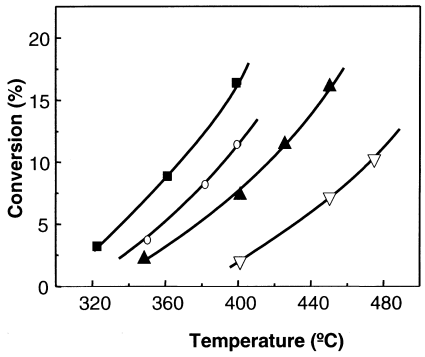

Fig. 1. Variation of the conversion of ethane with the reaction temperature during the oxidation of ethane on Cr- and Ga-containing catalysts. Ga/(Ga+Cr) atomic ratios of: 0 (■); 0.3 (○); 0.4 (▲) and 0.7 (▽).

flow of Ar/H_2 (40 cm^3 min^{-1}, 10% of H_2) and heating at 10°C min^{-1}. The water produced in the reduction reaction was eliminated by passing the gas flow through a cold finger (−80°C). The consumption of reductor was controlled by an on-line chromatograph provided with TC detector.

2.3. Catalytic tests

The catalytic tests for the oxidative dehydrogenation of ethane were carried out in a fixed-bed quartz tubular reactor (16 mm i.d., 500 mm length) equipped with a coaxial thermocouple for measuring the temperature profiles. Catalyst samples from 0.05 to 0.5 g (particle size between 0.42 and 0.59 nm) were mixed with variable amounts of SiC to keep a constant volume in the catalyst bed of 3 cm^3. The catalysts were calcined at 500°C for 4 h using the same feed employed in the catalytic test. The reaction was studied in the 350°C–500°C temperature interval, using an ethane/oxygen/helium molar ratio of 10/5/85. The total flow was varied from 3 to 12 l h^{-1} to obtain different contact times (W/F). Analysis of reactants and products was carried out using gas chromatography, and two different columns: (i) Porapak Q (3.0 m × 1/8 in.); (ii) Molecular Sieve 5A (1.5 × 1/8 in.). Blank runs in the studied temperature interval were carried out using pure SiC, at the lowest total flow used in this study (3 l h^{-1}). Under our reaction conditions the presence of homogeneous reaction can be neglected.

3. Results

3.1. Oxidative dehydrogenation of ethane

A new family of catalysts based on gallium oxide/chromia-pillared α-zirconium phosphate, with 0/100, 30/70, 40/60 and 70/30 Ga/Cr atomic ratios, have been tested in the oxidative dehydrogenation of ethane. Another mixed alumina/chromia α-zirconium phosphate has been included in this study for comparison. Fig. 1 shows the variation of the ethane conversion with the reaction temperature of Ga/Cr-containing catalysts. It can be seen that the ethane

Table 2
Catalytic behaviour of the studied pillared phosphates in the oxidative dehydrogenation of ethane at 400°C

Catalyst	W/F[a]	Conversion (%)	Selectivity (%)			r^{b}_{C2H6}	TOF[c]
			Ethene	CO	CO_2		
Ga/Cr-0/100	5.0	10.0	12.0	34.1	53.9	1.996	2.61
Ga/Cr-30/70	8.5	11.5	23.6	31.5	43.4	1.348	2.29
Ga/Cr-40/60	8.5	7.4	25.0	31.3	43.7	0.868	2.13
Ga/Cr-70/30	35	3.6	21.0	21.4	48.2	0.102	0.46
Al/Cr-40/60	8.5	5.4	23.9	33.2	42.6	0.636	1.92

[a] In g_{cat} h (mol C_2)$^{-1}$.
[b] Rate of propane oxidation in 10^2 mol C_2 g^{-1}_{cat} h^{-1}.
[c] Turnover frequency in mol C_2 h^{-1} mol^{-1}_{Cr}.

conversion decreases when the Ga content increases. Table 2 shows the reactivities for the ethane oxidation at 400°C along the group of catalysts and the selectivities to the main reaction products.

The rate of ethane conversion ($r_{C_2H_6}$) decreases with decreasing Cr content, indicating that Cr(III) atoms are the active centers in this reaction (Table 2). Conversion of the activity data to turnover frequency (TOF, considering only the activity of Cr atoms) reveals that, except for the sample with low Cr content (Ga/Cr-70/30), similar values were observed in all cases.

Note that ethene, CO and CO_2 were the main products observed during the oxidation of ethane on our catalysts. O-containing products other than carbon oxides were not observed. Fig. 2 shows the variation of the selectivity to ethene with the reaction temperature. The selectivity to ethene decreases with the reaction temperature on Ga-free catalyst. However, an opposite trend is observed on Ga-containing catalysts. Thus, it appears that the presence of Ga on the catalyst favors a promoter effect on the selectivity to ethene.

Fig. 3 shows the variation of the selectivity to ethene with the catalyst composition, achieved at 400°C and an ethane conversion of 10%. It can be seen that better selectivity to ethene was achieved at a Ga/(Ga + Cr) content of 0.4.

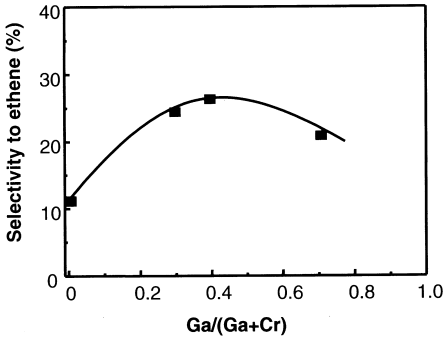

Fig. 2. Variation of the selectivity to ethene with the reaction temperature during the oxidation of ethane on Cr- and Ga-containing catalysts. Experimental conditions and symbols same as in Fig. 1.

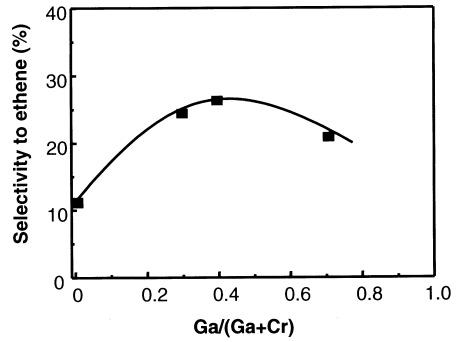

Fig. 3. Variation of the selectivity to ethene with the Ga/(Ga + Cr) atomic ratios of catalysts at 400°C and ethane conversion of 10%.

However, we must indicate that the selectivity to ethene also depends on the reaction temperature. Thus, the results shown in Fig. 4 indicate that, at the same ethane conversion, the selectivity to ethene increases with the reaction temperature.

To study the influence of different metals, Fig. 5 shows the variation of the ethane conversion with the reaction temperature on Cr-, Ga/Cr-, and Al/Cr-containing catalysts. It can be seen that the catalytic activity decreases as follows: Cr- ≫ Ga/Cr- > Al/Cr-containing materials. However, the selectivity to ethene shows a different trend. Thus, from the results presented in Fig. 6 it can be concluded that the selectivity to ethene decreases as follows: Ga/Cr- > Al/Cr- ≫ Cr-containing materials.

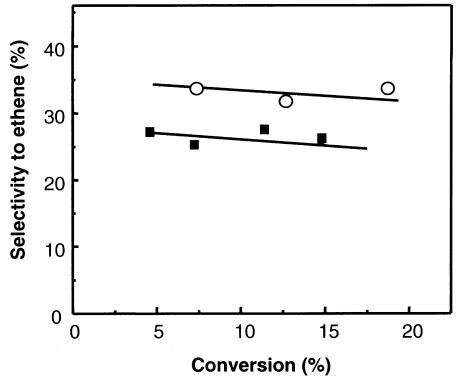

Fig. 4. Variation of the selectivity to ethene with the ethane conversion during the oxidation of ethane on the Ga/Cr-40/60 sample at 400 (■) and 475°C. (○).

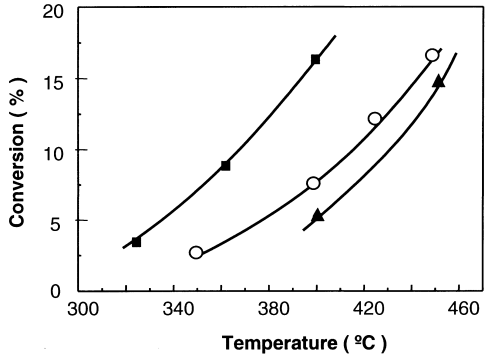

Fig. 5. Variation of the conversion of ethane with the reaction temperature during the oxidation of ethane on: Ga/Cr-0/100 (■); Ga/Cr-40/60 (○) and Al/Cr-40/60 (▲).

3.2. Characterization of catalysts

In all the catalysts studied, the surface Cr/Zr atomic ratios, obtained by XPS, agree very well with the bulk Cr/Zr ratios obtained by chemical analysis. The chromium contents for Ga/Cr–ZrP catalysts range between 11.5 and 39.7 wt.%. This result indicates that no surface segregation of the metallic oxides in all the studied composition ranges takes place during the synthesis or calcination of these catalysts. By this technique, Cr(III), with B.E. ranged between 576.5 and 577 eV, was the only chromium species observed in all catalysts. On the other hand, the specific surface areas are related to the chromium loading and decrease along the series

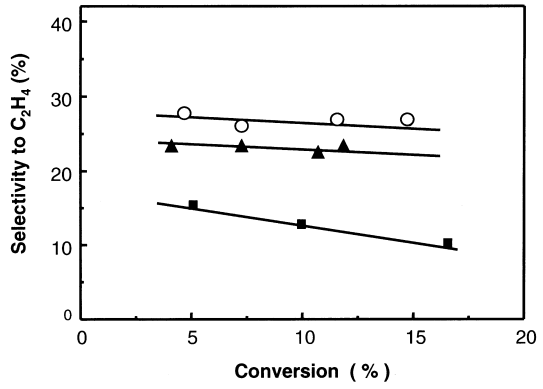

Fig. 6. Variation of the selectivity to ethene with the ethane conversion during the oxidation of ethane on: Ga/Cr-0/100 (■); Ga/Cr-40/60 (○) and Al/Cr-40/60 (▲) at 400°C.

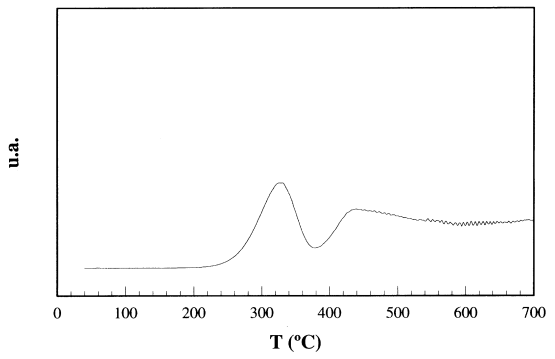

Fig. 7. TPR pattern of sample Ga/Cr-40/60.

from 426 $m^2\ g^{-1}$ up to 257 $m^2\ g^{-1}$. These solids are quite microporous with a micropore volume of 0.25–0.1 $cm^3\ g^{-1}$ along the series. In general, Al/Cr-40/60 catalyst, with a similar chromium content to the sample Ga/Cr 40/60–ZrP, also exhibits similar textural properties.

Fig. 7 shows the TPR pattern of sample Ga/Cr-40/60. The presence of a peak at 327°C corresponds to the reducible Cr atoms. Comparing the reducibility of samples with different Cr content (considering the temperature in which a maximum H_2 uptake is obtained), it can be seen that this decreases according to: Ga/Cr-70/30 (336°C) > Ga/Cr-40/60 (327°C) > Ga/Cr-

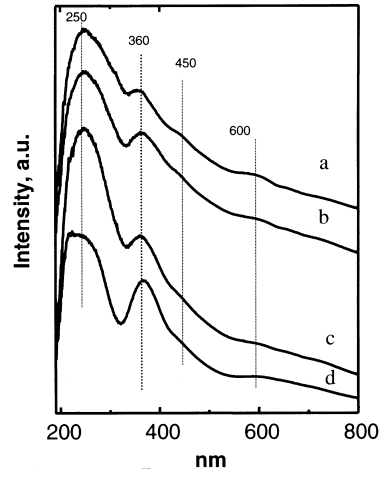

Fig. 8. Diffuse reflectance spectra in the UV–vis region of Cr- and Ga-containing catalysts before activation. Ga/(Ga+Cr) atomic ratios of: (a) 0; (b) 0.3; (c) 0.4; and (d) 0.7.

30/70 (323°C). Consequently, the incorporation of Ga^{+3} ions to the Cr_2O_3 nanoparticles seems to stabilize chromium species against redox properties.

Diffuse reflectance spectra in the UV–vis region before and after the catalytic test are shown in Figs. 8 and 9. In all cases, the spectra are characterized by the presence of bands at 250, 360, 442 and 584 nm. The bands at 360, 442 and 584 nm correspond to $^4A_{2g} \rightarrow {}^4T_{1g}$, $^4A_{2g} \rightarrow {}^4T_{1g}$ and $^4A_{2g} \rightarrow {}^4T_{2g}$ transitions typical of Cr^{3+} in octahedral environment [26,31]. These bands are present in all catalysts (before and after the catalytic test). Another intense band at 250 nm is due to charge transfer in Cr(VI) in tetrahedral coordination. The intensity of this band decreases with the gallium loading. This effect is also after the catalytic tests. Thus, these results reveal that if some Cr(VI) atoms are present on the surface of catalysts, they present a low concentration which is not detectable by XPS measurements.

All solids present acid sites as inferred from NH_3-TPD data with total acidity values higher than 1633 μmol g^{-1} for Ga/Cr–ZrP catalysts. In addition, IR studies of adsorbed pyridine reveal that although both types of acid site are present, the number of Lewis acid sites largely decreases along the group of catalysts as the gallium content increases. This effect is more pronounced in the case of Al/Cr-40/60 sample. On the other hand, these acid solids are also active in the dehydration of 2-propanol. However, the catalytic activity depends on the chemical composition. Thus, the activities range between 17.4 and 13.7 μmol g^{-1} s^{-1} when the Cr^{3+} is partially substituted by Ga^{3+}.

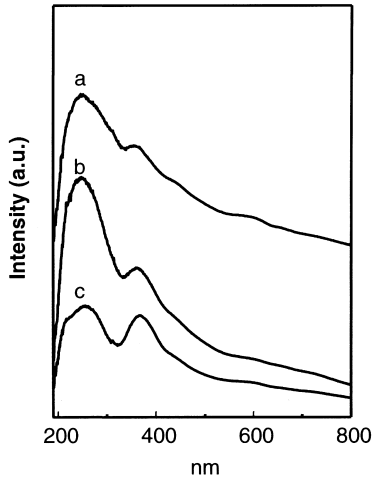

Fig. 9. Diffuse reflectance spectra in the UV–vis region of Cr- and Ga-containing catalysts after catalytic tests: (a) Ga/Cr-0/100; (b) Ga/Cr-40/60; and (c) Al/Cr-40/60.

4. Discussion and conclusions

The catalytic results for the OXDH of ethane indicate that the catalytic activity of Cr-containing catalysts depends on the Cr content and is independent of the presence of Ga or Al. However, except in the case of sample Ga/Cr-70/30, the catalysts show low decreases in their TOF when the Cr content decreases. Since TPR results indicate that the reducibility decreases with the amount of Ga incorporated, it can be concluded that the active sites in these catalysts are Cr atoms, and their activities depend on their redox properties. This trend has also been observed on other active and selective catalysts for the OXDH of ethane [2,30].

On the other hand, the selectivity to ethene for the OXDH of ethane could be related to the nature and strength of acid sites. In fact, it has been proposed that the presence of acid sites near redox sites could influence the selectivity to ethene from ethane since these acid sites could also favor a fast desorption of olefin intermediates. However, the nature of acid sites could also influence the rate of olefin formation.

If we compare the trend of the selectivity to ethene with the ethane conversion (Fig. 6) it can be seen that the higher difference between both Ga- and Al-containing catalysts and Cr/Ga-0/100 samples is the higher selectivity to ethene at high ethane conversions in the first two cases. It has been suggested that Brönsted acid centers are inactive in the OXDH of propane [22]. As mentioned above, Ga/Cr-0/100 catalyst is the most acidic material and also exhibits the maxi-

mum number of Lewis acid sites (Table 1). When gallium ions are incorporated into the network of pillaring oxides the number of acid sites of the resulting materials not only decreases, but the number of redox centers, too. In consequence Ga/Cr-0/100 sample with the maximum of redox and acid centers is the most active catalyst, but show lower selectivity owing to the olefin intermediates that are strongly retained and suffer ulterior oxidation. However, samples containing gallium present a lesser number of acid sites and furthermore a lower strength, as can be inferred from the lower remaining concentration of Lewis acid sites in these samples after evacuation at 220°C with respect to the Ga/Cr-0/100 (Table 1). Thus, olefin intermediates will be easily desorbed from these sites. On the other hand, TPR studies demonstrated that the oxidative power of catalysts decreases in samples containing gallium. Therefore, it can be concluded that redox centers surrounded by acid sites with intermediate strength are preferred for this oxidative reaction of ethane. This assumption is confirmed in the experiment investigating the influence of different metals. In fact, although the order of activities found was $Cr > Ga/Cr > Al/Cr$, which matches very well with the total concentration of Lewis acid sites, the order of selectivities found is $Ga/Cr > Al/Cr > Cr$, which agrees very well with the strength of these acid sites. Therefore, the less acidic sites (Ga ions) provoke the highest selectivity (Fig. 6).

In conclusion, Cr-containing oxides pillared zirconium phosphate materials are active catalysts for the oxidative dehydrogenation of ethane and the catalytic activity was observed to be proportional to the number of redox cations, Cr(III), although they present low selectivities to ethane. Moreover, the partial substitution of chromium cations by gallium or aluminium favors a better selectivity to ethane, probably as a consequence of the effect that these vicary ions exert on both the oxidizing power of chromium species and the acid strength of acid sites. Furthermore, an important conclusion is that optimum performance of this new kind of chromium catalysts is attained at very low temperature, only 400°C–450°C. In this conditions, Ga/Cr-40/60 catalyst for instance, shows a yield of ethene of 4.4 at a reaction temperature of 450°C.

Acknowledgements

Financial support from DGICYT, Spain (Projects MAT97-0561 and MAT97-906) is gratefully acknowledged.

References

[1] A. Parmaliana, V. Sokolovskii, D. Miceli, N. Giordano, Appl. Catal., A 135 (1996) L1.
[2] A. Corma, J.M. López-Nieto, N. Paredes, J. Catal. 144 (1993) 425.
[3] X. Gao, P. Ruiz, Q. Xim, X. Guo, B. Delmon, J. Catal. 148 (1994) 56.
[4] P. Concepción, J.M. López-Nieto, J. Pérez-Pariente, , J. Mol. Catal. 99 (1995) 173.
[5] J.G. Eon, P.G. Pries de Oliveira, F. Lefebvre, J.C. Volta, in: V. Cortés-Corberán, S. Vic-Bellón (Eds.), New Developments in Selective Oxidation II, Elsevier, Amsterdam, 1994, p. 83.
[6] B. Grzybowska, P. Mekss, R. Grabowski, K. Wcislo, Y. Barbaux, L. Gengembre, in: V. Cortés-Corberán, S. Vic-Bellón (Eds.), New Developments in Selective Oxidation II, Elsevier, Amsterdam, 1994, p. 151.
[7] N. Boisdron, A. Monnier, L. Jalowiecki-Uhamel, Y. Barbaux, J. Chem. Soc. Faraday Trans. 91 (1995) 2899.
[8] A. Corma, J.M. López-Nieto, N. Paredes, M. Pérez, Appl. Catal., A 97 (1993) 159.
[9] U. Schart, M. Scharmi-Marth, A. Wokaun, A. Baiker, J. Chem. Soc. Faraday Trans. 87 (1991) 3299.
[10] H.K. Matralis, M. Ciardelli, M. Ruwet, P.J. Grange, J. Catal. 157 (1995) 368.
[11] J.M. López-Nieto, A. Dejoz, M.I. Vázquez, Appl. Catal., A 132 (1995) 41.
[12] T. Lindblad, B. Rebenstorf, Z. Yan, S.L.T. Anderson, Appl. Catal., A 112 (1994) 187.
[13] T. Blasco, P. Concepción, J.M. López-Nieto, J. Pérez-Pariente, J. Catal. 152 (1995) 1.
[14] T. Blasco, J.M. López-Nieto, Appl. Catal., A 157 (1997) 117.
[15] E.A. Mamedov, V. Cortés-Corberán, Appl. Catal., A 127 (1995) 1.
[16] P. Olivera-Pastor, P. Maireles-Torres, E. Rodríguez-Castellón, A. Jiménez-López, T. Cassagneau, D.J. Jones, J. Rozière, Chem. Mater. 8 (1996) 1758.

[17] A. Corma, Chem. Rev. 97 (1997) 2373.
[18] F.J. Pérez-Reina, E. Rodríguez-Castellón, A. Jiménez-López, Langmuir 15 (1999) 2047.
[19] F.J. Pérez-Reina, E. Rodríguez-Castellón, A. Jiménez-López, submitted to Langmuir.
[20] P. Olivera-Pastor, J. Maza-Rodríguez, P. Maireles-Torres, E. Rodríguez-Castellón, A. Jiménez-López, J. Mater. Chem. 4 (1994) 179.
[21] M. Alcántara-Rodríguez, P. Olivera-Pastor, E. Rodríguez-Castellón, A. Jiménez-López, M. Lenarda, L. Storaro, R. Ganzerla, J. Mater. Chem. 8 (1998) 1625.
[22] M. Alcántara-Rodríguez, E. Rodríguez-Castellón, A. Jiménez-López, Langmuir 15 (1999) 1115.
[23] R. Grabowski, B. Grzybowska, K. Samsom, J. Sloczynski, K. Wcislo, React. Kinet. Catal. Lett. 57 (1996) 127.
[24] J. El-Idrissi, M. Kacimi, F. Bozon-Verduraz, M. Ziyad, Catal. Lett. 56 (1999) 221.
[25] M. Loukah, G. Coudurier, J.C. Vedrine, Stud. Surf. Sci. Catal. 72 (1992) 191.
[26] M. Loukah, G. Coudurier, J.C. Vedrine, M. Ziyad, Microporous Mater. 4 (1995) 345.
[27] G. Alberti, E. Torraca, J. Inorg. Nucl. Chem. 30 (1968) 317.
[28] F.J. Pérez-Reina, P. Olivera-Pastor, P. Maireles-Torres, E. Rodríguez-Castellón, A. Jiménez-López, Langmuir 14 (1998) 4017.
[29] J. Dakta, A.M. Turek, J.M. Jehng, I.E. Wachs, J. Catal. 135 (1992) 186.
[30] F. Cavani, F. Trifiro, Catal. Today 24 (1995) 307.
[31] A.B.P. Levo, in: Inorganic Electronic Spectroscopy, 1984, p. 417, Amsterdam.